NJC

Accepted Manuscript

This article can be cited before page numbers have been issued, to do this please use: Q. Meng, Y. Wang, H. Feng, F. Zhou, B. Zhou, C. Wang, R. Zhang and Z. Zhang, *New J. Chem.*, 2018, DOI: 10.1039/C7NJ04107A.

ROYAL SOCIETY OF CHEMISTRY

rsc.li/njc

View Article Online
DOI: 10.1039/C7NJ04107A

Journal Name

ARTICLE

A novel glucosamine-linked fluorescence chemosensor for the detection of pyrophosphate in aqueous medium and live cells

Received 00th January 20xx,

Accepted 00th January 20xx

DOI: 10.1039/x0xx00000x

www.rsc.org/

Qingtao Meng,*[a] Yue Wang,[a] Huan Feng,[a] Fang Zhou,[a] Bo Zhou,[a] Cuiping Wang,[a] Run Zhang[a,b] and Zhiqiang Zhang*[a]

There is a growing interest in monitoring the level of pyrophosphate (PPi) in biological processes due to its significant roles in live organisms. In this paper, we described a Cu^{2+} ensemble based chemosensor (**GN**-Cu^{2+}) for highly selective detection of PPi in aqueous medium and live cells. The fluorescence silent ensemble, **GN**-Cu^{2+} was facilely prepared by complexing of the glucosamine-1,8-naphthalimide fluorescent ligand (**GN**) with paramagnetic Cu^{2+}. The structure of **GN** was confirmed by ^{1}H NMR, ^{13}C NMR and high-resolution mass spectroscopy (HRMS) assays. The spectroscopic characteristics of **GN**-Cu^{2+} were verified in detail through fluorescence emission and UV-vis spectra titration. The decomplexation of **GN**-Cu^{2+} by PPi led to the liberation of the fluorescent ligand, **GN**, and thus the fluorescence was switched on. Spectroscopic studies revealed that **GN**-Cu^{2+} possesses excellent tolerance to various anions and even other phosphate series, such as AMP, ADP, ATP, and inorganic phosphate (Pi). Detection limit for PPi was calculated to be 1.0 μM. **GN**-Cu^{2+} features several advantages, such as high selectivity, reliability at physiological pH and low cytotoxicity. Intracellular fluorescence imaging measurements indicated that **GN**-Cu^{2+} is cell membrane permeable and has been successfully used for detection of PPi in live MD-AMB-231 cells.

Introduction

Phosphate anion species, as one types of most important anions in biological systems, play essential role in living organisms.[1] Particularly the pyrophosphate (PPi) exists in biological systems at high level, serving many important roles in metabolism of living organisms.[2] For example, PPi is involved in many enzyme-catalyzed biosynthesis and metabolic processes, most of which produce PPi as a hydrolysis product of nucleoside polyphosphates such as ATP. [3] Beyond its physiological functions in biological systems, the abnormal concentration levels of PPi is also implicated in several diseases, such as arteriosclerosis and osteoarthritis.[4] For example, an elevated PPi concentration in the synovial fluid is associated with calcium pyrophosphate dihydrate crystal deposition disease and a condition called chondrocalcinosis.[5] However, the relative lack of PPi will result in medial calcification (also known as Mönckeberg's arteriosclerosis).[6] Furthermore, it has been reported that the intracellular PPi levels is also associated with the development of cancer, and thus being studied as the indicator for cancer.[7] Therefore, quantitative determination the concentration of PPi in a variety of biological environment has been emerged asa research topic recently.

Among various analysis methods,[8] fluorescent analysis using responsive chemosensor is particularly attractive due to their high sensitivity and selectivity, easy to fabricate, and non-destructive properties, especially the noninvasive analysis *in vivo* and *in vitro* imaging potential.[9] To date, by exploring several sensing mechanisms, a few PPi-specific fluorescence chemosensors have been synthesized and reported.[10] Among various chemosensors prepared for PPi, transition metal complex have been selected for the construction of fluorescence chemosensor because the structural and geometrical flexibility of metal centers can provide an excellent way of organizing anion binding groups.[11] This type of PPi chemosensor is usually designed based on the displacement approach, where a fluorophore–metal complex named the "ensemble" is general nonfluorescent due to metal-ion-induced fluorescence quenching. Since PPi has a stronger complexing ability to metal center, the addition of PPi to the ''ensemble'' may release the fluorophore into the solution, accompanied by the recovering of fluorescence.[12] In these assays, Al^{3+}, Zn^{2+} and Fe^{3+} are the most commonly used metal ions, and oxygen or nitrogen-rich organic compounds are usually employed as the fluorescent ligands.[13] It is well known that Cu^{2+} is a fluorescence quencher due to its notorious paramagnetic nature.[14] Furthermore, the resultant fluorescence sluggish Cu^{2+} ensemble can be potential applied as the selective fluorescence turn-on chemosensor *via* analyte

[a] School of Chemical Engineering, University of Science and Technology Liaoning, 185 Qianshan Zhong Road, Anshan 114044, P. R. China
E-mail: qtmeng@ustl.edu.cn; zhangzhiqiang@ustl.edu.cn, Tel: +86-421-5928009.
[b] Australian Institute for Bioengineering and Nanotechnology, The University of Queensland, Brisbane, 4072, Australia

Electronic Supplementary Information (ESI) available: [details of any supplementary information available should be included here]. See DOI: 10.1039/x0xx00000x

View Article Online
DOI: 10.1039/C7NJ04107A

induced Cu^{2+} displacement approach.[15] This kind of fluorescence enhancement ("OFF-ON") response mode is more desirable in sensing than the one with fluorescence quenching ("ON-OFF").[16] Although the advances of displacement-based approaches, PPi-specific fluorescent chemosensors based on Cu^{2+} ensemble have been scarcely reported.[17] In this work, we have designed and synthesized a glucosamine-linked fluorescent ligand (**GN**) based on 1,8-naphthalimide dye. The fluorescence of **GN** will be selectively quenched by paramagnetic Cu^{2+} *via* forming **GN**-Cu^{2+} ensemble. The specific interaction of PPi with **GN**-Cu^{2+} ensemble led to the liberation of fluorophore (**GN**) (Scheme 1), which could serve as fluorescence "turn on" chemosensor for PPi in aqueous medium and in living cells.

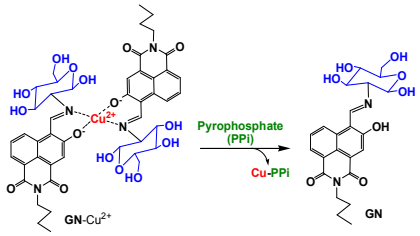

Scheme 1. Proposed response mechanism of **GN**-Cu^{2+} towards PPi.

Results and Discussion

Design, synthesis and characterization of GN-Cu^{2+} ensemble

The fluorescent ligand, **GN** was prepared by a one-step condensation reaction between 4-formyl-3-hydroxy-1,8-naphthalic-n-butylimide with glucosamine in methanol. The product was purified and the structure of **GN** was confirmed by ^{1}HNMR, ^{13}CNMR and HRMS (Fig. S1-3). 1,8-Naphthalimide dye was chosen as fluorophore owing to its excellent photochemical and photophysical properties, such as absorption and emission in visible range, high fluorescence quantum yield and superb stability against light.[18] Glucosamine moiety was introduced into **GN** molecule, which facilitate the water solubility, biocompatibility and the ability for tumor cell uptake.[19] The formation of **GN**-Cu^{2+} ensemble and its sensing performance towards PPi have been investigated in detail using the UV-vis spectra, fluorescence spectra and fluorescence imaging.

Spectroscopic characterization of GN-Cu^{2+} ensemble in solution

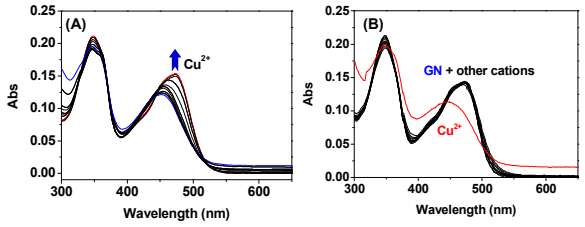

Fig. 1 (A) UV-vis absorption spectra of **GN** (10 μM) upon the addition of increasing amount of Cu^{2+} (0–50 μM) in 20 mM HEPES buffer (DMSO-H_2O = 1/9, v/v, pH 7.4). (B) UV-vis absorption spectra of **GN** (10 μM) in the presence of various cations (50 μM) in HEPES buffer.

The formation of **GN**-Cu^{2+} ensemble was firstly investigated by recording the changes in UV-Vis absorption and fluorescence spectra. As shown in Fig. 1A, the free fluorescent ligand, **GN** showed characteristic absorption maximums at 348 nm and 450 nm in 20 mM HEPES buffer (DMSO-H_2O = 1/9, v/v, pH 7.4), that can be attributed to the intramolecular charge transfer (ICT) transition of 1,8-naphthalimide unit.[20] Upon addition of Cu^{2+} to the solution of **GN**, the absorbance at 450 nm was found to be significantly red-shifted to 474 nm, indicating the complexation of **GN** with Cu^{2+}. No obvious changes in UV-vis absorption spectra was noticed by the addition of other competitive metal ions, including Li^{+}, K^{+}, Na^{+}, Ca^{2+}, Mg^{2+}, Ba^{2+}, Ag^{+}, Cd^{2+}, Pb^{2+}, Zn^{2+}, Ni^{2+}, Co^{2+}, Mn^{2+}, Hg^{2+}, Fe^{3+}, Cr^{3+}, and Al^{3+} (Fig. 1B). These results indicated that **GN** was a Cu^{2+}-specific fluorescent ligand.

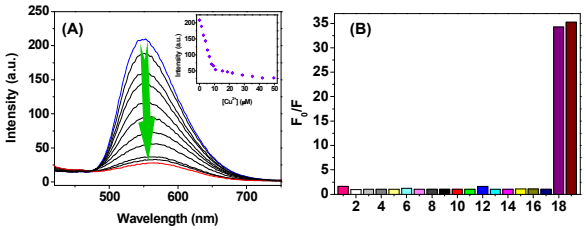

Fig. 2 (A) Fluorescence emission spectra of **GN** (10 μM) upon the addition of increasing amount of Cu^{2+} (0–50 μM) in 20 mM HEPES buffer (DMSO-H_2O = 1/9, v/v, pH 7.4). Inset: fluorescence intensities of **GN** (10 μM) at 550 nm as a function of Cu^{2+} (0–50 μM). (B) Fluorescence responses of **GN** (10 μM) in HEPES buffer in the presence of various cations (50 μM): 1. Li^{+}, 2. K^{+}, 3. Na^{+}, 4. Ca^{2+}, 5. Mg^{2+}, 6. Ba^{2+}, 7. Ag^{+}, 8. Cd^{2+}, 9. Pb^{2+}, 10. Zn^{2+}, 11. Ni^{2+}, 12. Co^{2+}, 13. Mn^{2+}, 14. Hg^{2+}, 15. Fe^{3+}, 16. Cr^{3+}, 17. Cu^{2+}, 18. Al^{3+}, 19. the mixture of all the canions (50 μM for each). The intensities were recorded at 550 nm, excitation at 450 nm.

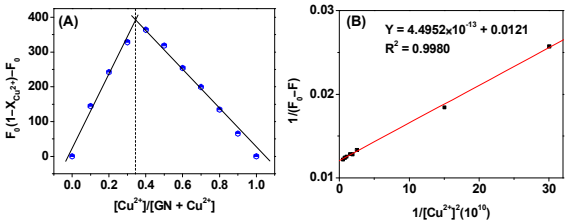

Fig. 3 (A) Job's plot of the reaction between **GN** and Cu^{2+} (total concentration was kept at 10 μM). (B) Benesi-Hildebrand plot (emission at 550 nm) of **GN** (10 μM) based on 2:1 binding stoichiometry with Cu^{2+}. Excitation was performed at 450 nm.

The complexation of **GN** with Cu^{2+} was then verified by analysis of fluorescence titration. **GN** displayed strong fluorescence at 550 nm in 20 mM HEPES buffer (DMSO-H_2O = 1/9, v/v, pH 7.4). As expected, the fluorescence intensity of **GN** decreased gradually with a 15 nm bathochromic-shift in the presence of incremental addition of Cu^{2+}. The fluorescence intensity reached to a constant value when 50 μM Cu^{2+} was added (Fig. 2A, inset). The results demonstrated the formation of **GN**-Cu^{2+} ensemble. It was found that the fluorescence of **GN** was exclusively quenched by Cu^{2+}. Asshownin Fig. 2B, nosignificant quenching of the fluorescence intensities observed in the presence of Fe^{3+}, Hg^{2+}, Cd^{2+}, Pb^{2+}, Zn^{2+}, Ni^{2+}, Co^{2+}, Mn^{2+}, Cr^{3+}, Ag^{+}, Ca^{2+}, Mg^{2+}, Ba^{2+}, Li^{+}, K^{+}, and Na^{+}. While

View Article Online
DOI: 10.1039/C7NJ04107A

the addition of 50 μM Cu^{2+} to the solution of **GN** coexisted with above cations giving rise to drastic quenching inaccordance with the addition of equal amounts of Cu^{2+} alone, indicating that Cu^{2+}-specific binding with **GN** was not disturbed by competitive ions. The binding stoichiometry of **GN** with Cu^{2+} was studied by Job's plot measurement. As shown in Fig. 3A, the fluorescence emission variation at 550 nm against the mole fraction of Cu^{2+} clearly showed a maximum level at 0.33 molecular fraction, which indicated the formation of the 2:1 stoichiometry complex between **GN** and Cu^{2+}.[21] Based on the 2:1 binding mode, the association constant (K_a) was evaluated to be 7.46×10^8 M^{-2} using the Benesi–Hildebrand method (Fig. 3B).[22]

Spectroscopic responses of GN-Cu^{2+} ensemble towards PPi

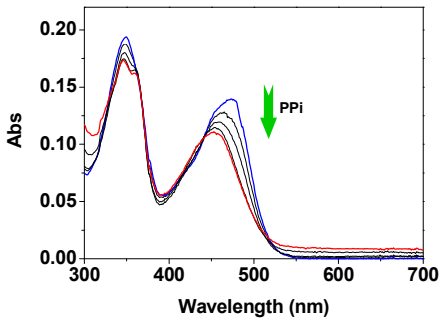

Fig. 4 UV-vis absorption spectra of **GN**-Cu^{2+} (10 μM) in 20 mM HEPES buffer (DMSO-H_2O = 1/9, v/v, pH 7.4) in the presence of different amounts of PPi (0–300 μM). Excitation was performed at 450 nm.

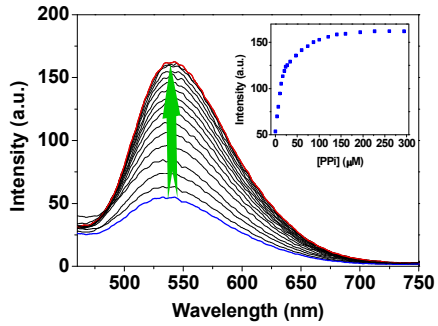

Fig. 5 Fluorescence spectra of **GN**-Cu^{2+} (10 μM) in 20 mM HEPES buffer (DMSO-H_2O = 1/9, v/v, pH 7.4) in the presence of different amounts of PPi (0–300 μM). Excitation was performed at 450 nm.

The high affinity of PPi towards Cu^{2+} insured **GN**-Cu^{2+} ensemble a candidate of fluorescence turn on chemosensor for PPi sensing by a simple displacement approach. Stock solution of **GN**-Cu^{2+} ensemble for PPi sensing was *in situ* prepared by the addition of 5.0 equiv. of Cu^{2+} to **GN** (10 μM) solution in 20 mM HEPES buffer (DMSO-H_2O = 1/9, v/v, pH 7.4). To investigate the responses of **GN**-Cu^{2+} ensemble upon exposure to PPi, UV–vis titration experiments were firstly conducted. As shown in Fig. 4, continuously added PPi into the solution of **GN**-Cu^{2+}, a reduction of the maximum absorption at 474 nm was concomitant with continuous hypsochromic shift, and saturation was reached when 300 μM PPi was added. The final absorption band was similar to the free **GN** at identical conditions, indicating that the liberation of fluorescent ligand **GN** induced by PPi.

The sensing performance of **GN**-Cu^{2+} towards PPi in aqueous solution was further examined by the fluorescence spectra measurements. **GN**-Cu^{2+} presented a weak fluorescence emission in 20 mM HEPES buffer (DMSO-H_2O = 1/9, v/v, pH 7.4). Upon the addition of PPi, the fluorescence intensity increased gradually (Fig. 5). Maximum fluorescence intensity was obtained when 30 equiv. of PPi was added (Fig. 5 inset). The emission spectrum of the solution is essentially identical with the emission of free **GN**, indicating that the decomplexing of Cu^{2+} by PPi. The relative fluorescence intensity of **GN**-Cu^{2+} is linearly proportional to the concentration of PPi in the range of 0-20 μM (Fig. S4). The fluorescence detection limit for PPi was calculated to be 1.0 μM according to the methods defined by IUPAC.[23] To verify the replacement of **GN** by PPi, the binding mode of **GN**-Cu^{2+} toward PPi was determined by using the Benesi–Hildebrand equation. As shown in Fig. S5, the plotting of $1/(F - F_0)$ versus 1/[PPi] showed a good linear relationship (R^2 = 0.9836), which indicates a stable 1:1 stoichiometry complexation species, and theassociation constant K_a was calculated to be 2.0×10^4 M^{-1}. The results further indicated that the coordination-induced ligand replacement mechanism is responsible for the spectroscopic responses towards PPi.

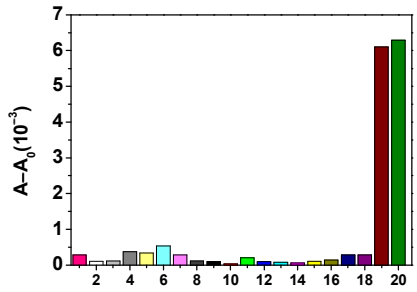

Fig. 6 Normalized absorbance responses of **GN**-Cu^{2+} (10 μM) in 20 mM HEPES buffer (DMSO-H_2O = 1/9, v/v, pH 7.4) in the presence of various analytes (300 μM): 1. CH_3COO^-, 2. CO_3^{2-}, 3. F^-, 4. SO_4^{2-}, 5. I^-, 6. S^{2-}, 7. Cl^-, 8. OH^-, 9. ClO^-, 10. SCN^-, 11. Br^-, 12. NO_3^-, 13. HSO_4^-, 14. NO_2^-, 15. Pi. 16. AMP, 17. ADP, 18. ATP, 19. PPi, 20. PPi co-existed with competitive anions.

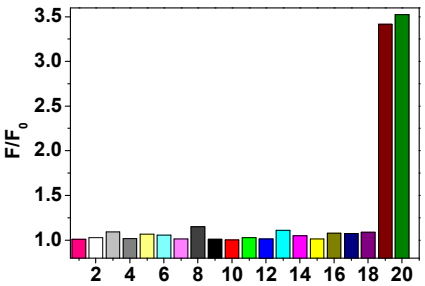

Fig. 7 Normalized emission responses of **GN**-Cu^{2+} (10 μM) in 20 mM HEPES buffer (DMSO-H_2O = 1/9, v/v, pH 7.4) in the presence of various analytes (300 μM): 1. CH_3COO^-, 2. CO_3^{2-}, 3. F^-, 4. SO_4^{2-}, 5. I^-, 6. S^{2-}, 7. Cl^-, 8. OH^-, 9. ClO^-, 10. SCN^-, 11. Br^-, 12. NO_3^-, 13. HSO_4^-, 14. NO_2^-, 15. Pi. 16. AMP, 17. ADP, 18. ATP, 19. PPi, 20. PPi co-existed

View Article Online
DOI: 10.1039/C7NJ04107A

with competitive anions. The intensities were recorded at 550 nm, excitation at 450 nm.

Spectroscopic titration experiments were further carried out to evaluate the selectivity of **GN**-Cu^{2+} ensemble to PPi. The absorbance responses of **GN**-Cu^{2+} to PPi were firstly examined by the addition of diverse anions, including CH_3COO^-, CO_3^{2-}, F^-, SO_4^{2-}, I^-, S^{2-}, Cl^-, OH^-, ClO^-, SCN^-, Br^-, NO_3^-, HSO_4^-, NO_2^-, PPi and other phosphate series, such as AMP, ADP, ATP, inorganic phosphate (Pi). Among these anions, only the addition of PPi led to a conspicuous change in the absorbent of the **GN**-Cu^{2+} (Fig. 6). To further confirm the selectivity of **GN**-Cu^{2+} ensemble for PPi, titration analysis by recording the changes of fluorescence spectra was performed. As shown in Fig. 7, clear enhancement in fluorescence intensity was observed by the addition of PPi, over other anions. These results indicated that **GN**-Cu^{2+} is selective for PPi among these anions under simulated physiological conditions.

Effect of pH

In view of the electrostatic force and metal coordination interaction could be varied by the pH conditions of the medium solution,[24] the effect of pH on the fluorescence response of **GN**-Cu^{2+} ensemble towards PPi was then investigated. As shown in Fig. 8, **GN** exhibited stable fluorescence intensity at a pH range from 4.0 to 11.0. A slight decrease of the emission spectra was observed less than pH 5.0, which was attributed to the protonation of the nitrogen atomon imine moiety. As expected, the emission intensity of **GN** in the presence of Cu^{2+} decreased obviously from pH 5.0 to 10.5, indicating that the coordination between **GN** and Cu^{2+}. Furthermore, no significant quenching in the fluorescence intensity was observed once the pH exceeds 10.5, which reflected that the higher pH could be well explained by the formation of $Cu(OH)_2$ and thus reducing the concentration of **GN**-Cu^{2+}. The results indicate that **GN**-Cu^{2+} ensemble were suitable for application under physiological conditions.

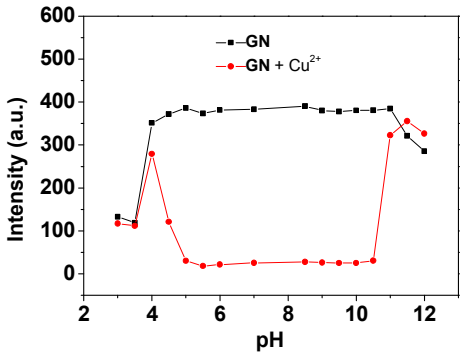

Fig. 8 Fluorescence spectra of **GN** and **GN**-Cu^{2+} as a function of pH values (3.0–12.0) in mixed aqueous solution (DMSO:H2O, 1:9, v/v).

Bioimaging application of GN-Cu^{2+} ensemble in live cells

Encouraged by the desirable features such as high selectivity, reliability at physiological pH, the capability of **GN**-Cu^{2+} to image PPi in living cells was evaluated. Prior to the microscopy imaging application in live cells, the long-term cytotoxicity of **GN**-Cu^{2+} to the human breast carcinoma cell line MDA-MB-231 was evaluated using the MTT assay method.[25] Fig. 9 presented the results of MD-AMB-231 cells incubated with different concentrations of **GN**-Cu^{2+} (0, 2, 8, 10, 20 and 50 μM) for 24 h. MD-AMB-231 cells viabilities remained approximately at 90% even at the high concentration of 50 μM for 24 h. The low cytotoxicity of **GN**-Cu^{2+} could be attributed to the introduction of glucosamine moiety on the **GN** molecule.

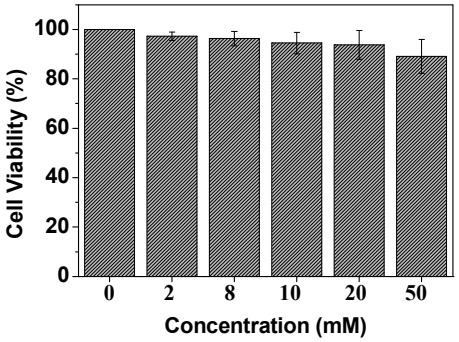

Fig. 9 Cell viability values (%) estimated by MTT assays after incubation with different concentrations of **GN**-Cu^{2+}.

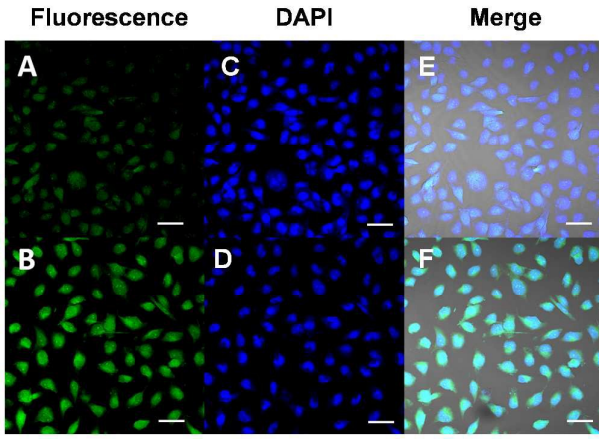

Fig. 10 DIC and confocal fluorescence and merged images of MD-AMB-231 cells were stained with DAPI and **GN**-Cu^{2+}, respectively. (A) MDA-MB-231 cells incubated with **GN**-Cu^{2+} (5 μM) only, (B) MDA-MB-231 cells pre-incubated with **GN**-Cu^{2+} (5 μM) followed by 0.1 mM PPi, (C) cells were stained with both DAPI and 5 μM **GN**-Cu^{2+}; (D) cells of (C) further incubated with PPi (0.1 mM) for another 30 min, (E) and (F) were merged images. Scale bar, 30 μm.

Having demonstrated the low cytotoxicity, reliability at physiological pH of **GN**-Cu^{2+} ensemble, we then studied the ability of **GN**-Cu^{2+} for the fluorescence imaging of PPi in living cells. MDA-MB-231 cells were incubated with 5 μM **GN**-Cu^{2+} for 30 min at 37 °C in a CO_2 incubator (95% relative humidity, 5% CO_2). Then the cells were washed with HEPES buffer for three times for microscopic imaging. As shown in Fig. 10 (A), the **GN**-Cu^{2+}-stained cells displayed weak green fluorescence, demonstrating that **GN**-Cu^{2+} features high cell-membrane permeability. Upon further incubation with 0.1 mM PPi, the

DOI: 10.1039/C7NJ04107A

green fluorescence in the cells was lightened arising from the liberation of fluorescent ligand, **GN** inside the cells (Fig. 10B). Overlay of confocal images of **GN**-Cu^{2+} and DAPI (4',6-diamidino-2-phenylindole) (Fig. 10C, D) showed that the fluorescence was evident distributed over the cells. The results demonstrated the capability of **GN**-Cu^{2+} ensemble for the analysis of PPi in live cells.

Experimental

Reagents and instruments

3-Hydroxy-1,8-naphthalic anhydride, hexamethylenetetramine (HMTA) and MTT (3-(4,5-dimethylthiazol-2-yl)-2,5-diphenyltetrazolium bromide) were purchased from Aladdin reagent Co. (Shanghai, China). D-Glucosamine hydrochloride, n-butylamine and trifluoroacetic acid were obtained from Sinopharm Chemical Reagent Co., Ltd. (China). Metal ions (nitrate salts) and anions (sodium salts) were purchased from Alfa Aesar. Unless otherwise stated, solvents and reagents were of analytical grade from commercial suppliers and were used without further purification.

^{1}H-NMR and ^{13}C-NMR spectra were recorded with an AVANCE600MHZ spectrometer (BRUKER) with chemical shifts reported as *ppm* (in DMSO, TMS as internal standard). High resolution mass spectra were recorded on an Agilent 6530 QTOF spectrometer. Fluorescence spectra were measured with Perkin Elmer LS55 luminescence spectrometer (USA). Absorption spectra were measured with a Perkin Elmer Lambda 900 UV/VIS/NIR spectrophotometer (USA). Quartz cuvettes with a 1 cm path length and 3 mL volume were involved in fluorescence and UV-vis spectrum measurements. The pH was recorded by OHAUS ST3100 digital pH-meter. Fluorescent images were obtained using an Olympus Fluoview FV 1000 IX81 inverted confocal laser-scanning microscope. The excitation wavelength was 405 nm. The images were analysis by Image J software version 1.44p

Preparation of stock solutions of cations and anions

Deionized water was used to prepare all aqueous solutions. A stock solution of **GN**-Cu^{2+} (0.5 mM) was prepared in dimethyl sulfoxide (DMSO), which was diluted with the mixture solution of 10 μM HEPES-buffered saline (DMSO-H_2O = 1:9, 20 mM, pH 7.4) prior to the spectral measurements. Solutions of a series of cations (nitrates salts, 20mM) and anions (sodium salts, 20mM) were prepared in deionized water. For pyrophosphate spectroscopic analysis, the measurement was performed immediately after the stock solutions were prepared.

Synthesis and characterization of the fluorescent GN

4-formyl-3-hydroxy-1,8-naphthalic-n-butylimide was papered according to the reported method.[20]

In a 100 mL round-bottom flask, D-glucosamine hydrochloride (0.216 g, 1.0 mmol) and triethylamine were dissolved in 15 mL methanol at 60 °C. The resulting solution was stirred for 10 min. Then, the solution of 4-formyl-3-hydroxy-1,8-naphthalic-n-butylimide (0.297 g, 1.0 mmol) in 25 mL methanol was added. The reaction mixture was then maintained at 60 °C for another 6 h to form orange precipitate. The crude product was filtered, washed with cooled methanol for three times to obtain **GN** in 88% yield. ^{1}H NMR (DMSO-*d*, 500 MHz) δ(*ppm*): 15.05 (s, 1H), 9.38 (s, 1H), 8.64 (d, *J* = 7.0 Hz, 1H), 8.19 (d, *J* = 6.05 Hz, 1H), 7.83 (t, *J* = 6.75 Hz, 1H), 7.78 (s, 1H), 7.17 (d, *J* = 5.2 Hz,1H), 5.56 (s, 1H), 5.25 (d, *J* = 4.5 Hz, 1H), 4.91 (t, *J* = 5.78 Hz, 1H), 4.69 (d, *J* = 4.8 Hz, 1H), 4.05 (d, *J*= 6.2 Hz, 2H), 3.81-3.59 (m, 6H), 3.29 (m, 2H), 1.65 (m, 2H), 1.40 (m, 2H), 0.98 (t, *J* = 6.15 Hz, 3H). ^{13}C NMR (DMSO-*d*, 125 MHz) δ(*ppm*): 170.7, 162.8, 162.3, 161.3, 132.2, 127.9, 126.9, 126.8, 124.7, 124.5, 122.0, 119.4, 109.5, 93.9, 76.2, 73.3, 70.6, 69.7, 60.3, 28.9, 19.1, 13.0. HRMS-API (negative mode, m/z) for [**GN**-H]$^{-}$: calcd 457.1616, found: 457.1807 [**GN**–H]$^{-}$; Found: 260.0995. m.p.: 177.2.2-178.8 °C.

Cytotoxicity assay

The cytotoxicity of **GN**-Cu^{2+} toward the human breast carcinoma cell line MDA-MB-231 was measured by methylthiazolyl tetrazolium (MTT) assay. MDA-MB-231 cells were seeded into a 96-well cell-culture plate at 1×10^{4} per well, and then incubated at 37 °C in a 5% CO_2 incubator. After 24 h, the culture medium was replaced with fresh medium containing **GN**-Cu^{2+}at concentrations of 0, 2, 8, 10, 20, 50 μM. Control wells were prepared by the addition of culture medium, and wells containing culture media without cells were used as blanks. The cells were incubated at 37°C under 5% CO_2 atmosphere for another 24 h. The culture medium with **GN**-Cu^{2+} was removed, and the cells were washed with PBS for three times. Then, 100 μL MTT solution (0.5 mg/mL) was added to each well of the 96-well, and the solution was incubated for another 4 h under the same conditions. The excess MTT solution was then carefully removed from each well, and the formed formazan was dissolved in 100 μL of DMSO (dimethyl sulfoxide). A TecanInnite M200 monochromator based multifunction microplate reader was used for measuring the OD570 (absorbance value) of each well referenced at 690 nm. The cell viability was calculate by the following formula: Vialibity (%) = (mean of absorbance value of treatment group–blank)/(mean absorbance value of control–blank) × 100.[26]

Fluorescence imaging of PPi in MDA-MB-231 cells

MDA-MB-231 cells were incubated with **GN**-Cu^{2+} (5 μM in cell culture medium, 0.5% DMSO) at 37 °C in a 5% CO_2 incubator. After 30 min, the cells were washed with HEPES buffer. The cells were imaged by confocal fluorescence microscopy. For detection of intracellular PPi, the cultured MDA-MB-231 cells in a T-75 flask were washed three times with HEPES buffer and then incubated with HEPES buffer containing 5 μM of **GN**-Cu^{2+} for 30 min at 37 °C in a 5% CO_2/95% air incubator. After washing three times with HEPES buffer, the cells were cultured for another 30 min with HEPES buffer containing 0.1 mM PPi. The cells were washed five times carefully with HEPES buffer and then subjected to the fluorescence imaging measurement. Fluorescence images were obtained using an Olympus Fluoview FV 1000 IX81 inverted confocal laser-scanning

View Article Online
DOI: 10.1039/C7NJ04107A

Conclusions

In summary, a 1,8-naphthalimide-based fluorescent chemosensing ensemble, **GN**-Cu^{2+}, has been developed for the highly selective detection of PPi in aqueous solution and living systems. In the presence of PPi, the effective snatching of Cu^{2+} from **GN**-Cu^{2+} ensemble, leading to the liberation of the fluorescent ligand, **GN**, and thus the fluorescence was switched on. **GN**-Cu^{2+} possesses excellent tolerance to biological anions and even other phosphate series, such as AMP, ADP, ATP, Pi. The modified glucosamine moiety on **GN** enhanced the water solubility, biocompatibility and tumor cell uptake. Low cytotoxicity of **GN**-Cu^{2+} was confirmed by the MTT assay. Confocal microscopy imaging studies revealed that **GN**-Cu^{2+} has potential as a powerful tool for the imaging of PPi in live cells. Given these promising results, we believe this contribution provides a new flexible strategy for the rational design of metal ensemble based chemosensors for the detection of anions in biological samples.

Acknowledgements

This work was supported by the Natural Science Foundation of Liaoning Province (No. 201602400), the Key Laboratory Program of Educational Department of Liaoning Province (No. LZ2015047) and National Natural Science Foundation of China (No. 21601076).

References

1 (a) P. Hu, S. Yang and G. Feng, *Org. Biomol. Chem*., 2014, **12**, 3701–3706; (b) M. Galizzi, J. M. Bustamante, J. Fang, K. Miranda, L. C. S. Medeiros, R. L. Tarleton and R. Docampo, *Mol. Microbiol*., 2013, **90**, 699–715; c) M. Stitt, *Botanica Acta*, 1998, **111**, 167–175; d) J.-H. Zhu, C. Yu, Y. Chen, J. Shin, Q.-Y. Cao and Jong S. Kim, *Chem. Commun*., 2017, **53**, 4342-4345.

2 (a) A. S. Rao, S. Singha, W. Choi and K, H, Ahn, *Org. Biomol. Chem*., 2012, **10**, 8410–8417; (b) W. N. Lipscomb and N. Strater, *Chem. Rev*., 1996, **96**, 2375–2433; c) P.-S. Yao, Z. Liu, J.-Z. Ge, Y. Chen and Q.-Y. Cao, *Dalton Trans*., 2015, **44**, 7470–7476.

3 E. Kittiloespaisan, I. Takashima, W. Kiatpathomchai, J. Wongkongkatep and A. Ojid, *Chem. Commun*., **2014**, *50*, 2126–2128.

4 a) H. Liu, R. Wei, Y. Xiang and A. Tong, *Anal. Methods,* 2015, **7**, 753–758; b) C.-T. Li, Y.-L. Xu, J.-G. Yang, Y. Chen, H. S. Kim, Q.-Y. Cao, J. S. Kim, *Sens. Actuat. B*, 2017, **251**, 617–623.

5 S.-Y. Jiao, K. Li, W. Zhang, Y.-H. Liu, Z. Huang, X.-Q. Yu, *Dalton Trans*. 2015, **44**, 1358–1365.

6 J. Wen, Z. Geng, Y. Yin, Z. Zhang and Z. Wang, *Dalton Trans*., 2011, **40**, 1984–198.

7 S. Lee, K. K. Y. Yuen, Katrina A. Jolliffe and J. Yoon, *Chem. Soc. Rev*., 2015, **44**, 1749–1762.

8 (a)D. H. Lee, J. H. Im, S. U. Son, Y. K. Chung and J. I. Hong, *J. Am. Chem. Soc*., 2003, **125**, 7752–7753; (b) J. Deng, P. Yu, L. Yang and L. Mao, *Anal. Chem*., 2013, **85**, 2516–2522; (c) J. G. March, B. M. Simonet, F. Grases, J. A. Munoz and M. Valiente, *Chromatographia*, 2003, **57**, 811–817; (d) B. K. Datta, S. Mukherjee, C. Kar, A. Ramesh and G. Das, *Anal. Chem*., 2013, **85**, 8369–8375; (e) I.-S. Shin, S. W. Bae, H. Kim and J.-I. Hong, *Anal. Chem*., 2010, **82**, 8259–8265; (f) L. Li, H. Li, G. Liu and S. Pu, *Luminescence*, 2017, DOI: 10.1002/bio.3347.

9 (a) Z. G. Yang, J. F. Cao, Y. X. He, J. H. Yang, T. Kim, X. J. Peng and J. S. Kim, *Chem. Soc. Rev*., 2014, **43**, 4563–4601; (b) S. Amatori, G. Ambrosi, M. Fanelli, M. Formica, V. Fusi, L. Giorgi, E. Macedi, M. Micheloni, P. Paoli, R. Pontellini, P. Rossi and M. A. Varrese, *Chem. Eur. J*., 2012, **18**, 4274–4284; (c) R. Zhang, B. Song, and J. Yuan, *Trends Anal. Chem.* 2018, **99**, 1-33.

10 (a) K. M. Kim, D. J. Oh and K. H. Ahn, *Chem. Asian J*., 2011, **6**, 122–127; (b) M. R. Ganjali, M. Hosseini, F. Aboufazeli, F. Faridbod, H. Goldooz and A. R. Badiei, *Luminescence*, 2012, **27**, 20–23; (c) N. Kumari, H. Huang, H. Chao, G. Gasser, Priv.-Doz, F. Zelder, *ChemBioChem*., 2016, **17**, 1211–1215; d) J.-Z. Ge, Z. Liu, Q.-Y. Cao, Y. Chen and J.-H. Zhu,*Chem. Asian J*., 2016, **11**, 687–690; e) H. K. Cho, D. H. Lee and J.-I. Hong, *Chem. Commun*., 2005, 1690-1692; f) N. K. Beyeh, I. Diez, M. Taimoory, D. Meister, A. Feig, J. F. Trant, R. H.A. Ras and K. Rissanen, *Chem. Sci*., 2017, 10.1039/C7SC05167K.

11 a) H. W. Rhee, H. Y. Choi, K. Han and J. I. Hong, *J. Am. Chem. Soc*., 2007, **129**, 4524–4525 ; b) S. Svane, F. Kjeldsen, V. McKee and C. J. McKenzie, *Dalton Trans*., 2015, **44**, 11877–11886 ; c) M. J. McDonough, A. J. Reynolds, W. Y. G. Lee and K. A. Jolliffe, *Chem. Commun*., 2006, 2971–2973 ; d) Z. Guo, W. Zhu and H. Tian, *Macromolecules*, 2010, **43**, 739–744 ; e) I.-S. Shin, S. W. Bae, H. Kim and J.-I. Hong, *Anal. Chem*., 2010, **82**, 8259-8365; f) W. Yu, J. Qiang, J. Yin, S. Kambam, F. Wang, Y. Wang and X. Chen, *Org. Lett*., 2014, **16**, 2220–2223.

12 (a) X. Lou, D. Ou, Q. Li and Z. Li, *Chem. Commun*., 2012, **48**, 8462–8477; (b) A. R. Chowdhury, B. G. Roy, S. Jana, T. Weyhermullere and P. Banerjee, *Sens. Actuators, B*, 2017, **241**, 706–715; (c) Z.-H. Fu, L.-B. Yan, X. Zhang, F.-F. Zhu, X.-L. Han, J. Fang, Y.-W. Wang and Y. Peng, *Org. Biomol. Chem*., 2017, **15**, 4115–4121; (d) R. Singh, A. Gogoi and G. Das, *RSC Adv*., 2016, **6**, 112246–112252; (e) D. Sarkar, P. Ghosh, S. Gharami, T. Kumar Mondal and N. Murmu, *Sens. Actuators, B*, 2017, **242**, 338–346; (f) O. G. Tsay, S. T. Manjare, H. Kim, K. M. Lee, Y. S. Lee and D. G. Churchill, *Inorg. Chem*., 2013, **52**, 10052–10061; (g) P. Wang, J. Wu, P. Su, C. Xu, Y. Ge, D. Liu, W. Liu and Y. Tang, *Dalton Trans*., 2016, **45**, 16246–16254; k) S. Bhowmik, B. N. Ghosh, V. Marjomäki and K. Rissanen,*J. Am. Chem. Soc*., 2014, **136**, 5543–5546.

13 (a) X. Su, C. Zhang, X. Xiao, A. Xu, Z. Xu and M. Zhao, *Chem. Commun*., 2013, **49**, 798–800; (b) G. Su, Z. Liu, Z. Xie, F. Qian, W. He and Z. Guo, *Dalton Trans*., 2009, 7888–7890.

14 (a) Y. H. Lee, N. Park, Y. B. Park, Y. J. Hwang, C. Kang and J. S. Kim, *Chem. Comm*., 2014, **50**, 3197–3200; (b) C. Kar, M. D. Adhikari, A. Ramesh and G. Das, *Inorg. Chem*., 2013, **52**, 743–752.

15 a) A. H. Malik, S.Hussain, A. S. Tanwar, S. Layek, V. Trivedi, P. K. Iyer, *Analyst*, 2015, **140**, 4388–4392; b) B. T. Nguyen, E. V. Anslyn, *Coord. Chem. Rev*., 2006, **250**, 3118–3127 ; c) A. Norouzy, Z. Azizi and W. M. Nau, *Angew. Chem., Int. Ed*., 2015, **54**, 792–795.

16 A. J. Moro, P. J. Cywinski, S. Körsten and G. J. Mohr, *Chem. Commun*.,2010, **46**, 1085–1087.

17 (a) K. S. Park, C. Y. Lee and H. G. Park, *Analyst*, 2014, **139**, 4691–4695; (b) A. H. Malik, S. Hussain, A. Sain Tanwar, S. Layek, V.Trivedi and P. K. Iyer, *Analyst*, 2015, **140**, 4388–4392.

18 J. Huang, Y. Xu and X. Qian, *Org. Biomol. Chem*., 2009, **7**, 1299–1303.

19 (a) A. V. Korotcov, Y. Ye, Y. Chen, F. Zhang, S. Huang, S. Lin, R. Sridhar, S. Achilefu and P. C. Wang, *Mol Imaging Biol*., 2012, **14**, 443–451; (b) W. Huang, P. Zhou, W. Yan, C. He, L. Xiong, F. Li and C. Duan, *J. Environ. Monit*., 2009, **11**, 330–335.

20 (a) S. K. Lee, M. G. Choi, J. Choi and S.-K. Chang, *Sens. Actuators, B*, 2015, **207**, 303–307; (b) H. Park and S.-K. Chang, *Sens. Actuators, B*, 2015, **220**, 376–380; c) S. Kumar Asthana, A. Kumar, Neeraj, K. K. Upadhyay, *Tetrahedron Lett*., 2014,

View Article Online
DOI: 10.1039/C7NJ04107A

55, 5988–5992; d) S. K. Kim, B.-G. Kang, H. S. Koh, Y. J. Yoon,S. J. Jung, B. Jeong, K.-D. Lee and J. Yoon, *Org. Lett*., 2004, **6**, 4655-4658; e) D. Wang, Y. Shiraishi and T. Hirai, *Chem. Commun*., 2011, **47**, 2673-2675.

21 a) X. X. Ren, Y. Wang, Q. T. Meng, H. M. Jia, Y. F. Wang, X. F. Kong, C. Y. Duan and Z. Q. Zhang, *ChemistrySelect*, 2016, **1**, 4397–4402; b) U. Reddy G., H. Agarwalla, N. Taye, S. Ghorai, S. Chattopadhyay, A. Das, *Chem. Commun*., 2014, **50**, 9899-9902; c) W. Hao, A. McBride, S. McBride, J. P. Gao and Z. Y. Wang, *J. Mater. Chem*., 2011, **21**, 1040–1048.

22 B. Peng, W. Chen, C. Liu, E. W. Rosser, A. Pacheco, Y. Zhao, H. C. Aguilar and M. Xian, *Chem. Eur. J*., 2014, **20**, 1010–1016.

23 L. Qiao, H. Nie, Y. Wu, F. Xin, C. Gao, J. Jing and X, Zhang, *J. Mater. Chem. B*, 2017, **5**, 525–530.

24 Z. Liu, C. Peng, Z. Lu, X. Yang, M. Pei and G. Zhang, *Dyes and Pigments*, 2015, **123**, 85–91.

25 (a) Y. Wang, X. Y. Wang, Q. T. Meng, H. M. Jia, R. Zhang, P. X. Zhu, R. F. Song, H. Feng and Z. Q. Zhang, *Tetrahedron*, 2017, **73**, 5700–5705; (b) Q. T. Meng, H. M. Jia, X. Gao, Y. Wang, R. Zhang, R. J. Wang and Z. Q. Zhang, *Chem. Asian J*., 2015, **10**, 2411–2418; (c) J. Ni and D. Hollander, J. Clin. *Lab. Anal*., 1996, **10**, 42–52.

26 (a) Q. M. Meng, Y. Shi, C. P. Wang, H. M. Jia, X. Gao,R. Zhang, Y. F. Wang and Z. Q. Zhang, *Org. Biomol. Chem*., 2015, **13**, 2918–2926; (b) X. Song, B. Dong, X. Kong, C. Wang, N. Zhang and W. Lin, *RSC Adv*., 2017, **7**, 15817–15822.